Progress In Electromagnetics Research B, Vol. 96, 19–38, 2022

A Compact Two-Port MIMO Antenna with Suppressed Mutual Coupling for IoT Applications

Rashmi Roges[1, 2, *], Praveen K. Malik[1], Sandeep Sharma[2], and Anita Gehlot[3]

Abstract—Compact antenna with good performance characteristics is always preferred for small IoT (Internet of Things) sensor nodes. The novelty of this proposed work is not in terms of design but in terms of application as Log-Periodic antennas has been so far used for UHF/VHF (Ultra High Frequency/Very High Frequency) and TV reception applications, and in this paper, the advantages of Log-Periodic structure have been exploited for IoT applications. This antenna design consists of two Log-Periodic like structured radiating elements on an FR4 substrate of 1.6 mm thickness. The compact antenna of size of 15 mm × 17 mm covers a bandwidth ranging from 2.01 GHz to 4.04 GHz including the WiMAX (2.3 GHz–2.4 GHz, 2.5 GHz–2.7 GHz and 3.4 GHz–3.6 GHz) and WLAN (2.4 GHz and 3.6 GHz) frequency bands. This system employs Defected Ground Structure (DGS) technique to obtain the required range of bandwidth of operation, for improving the isolation and obtaining mutual coupling suppression between the two individual elements. This miniaturized cheap antenna has a very low ECC (Envelope Correlation Coefficient) value and all other MIMO (Multiple Input Multiple Output) parameters in acceptable range. The isolation obtained over the entire range of operation is below −30 dB, and the performance efficiency is as good as 92.8% with a maximum gain of 2.9 dB. The simulated and measured results of the antenna system are also found to be in good agreement. The MIMO system can be considered as a good candidate for medium range IoT applications for its small size and good performance.

1. INTRODUCTION

The continuous evolution in the field of modern wireless system has pressurized the fast growth in the field of communication systems. The Internet of Things (IoT) technology has been gaining a lot of popularity recently. IoT is nothing but a connected chain of a huge number of heterogeneous devices over the Internet [1, 2]. A final communication standard has not yet been defined for IoT systems. So various communication standards and protocols have employed nowadays to serve the communication network of an IoT system on the basis of the requirement of the application [3]. Generally, IoT systems prefer compact devices with low data rates and low power consumption [4–7].

It is difficult that a single wireless technology would be able to meet the requirements of all IoT deployments. There will be a trade-off between the bandwidth, throughput, and the range of communication. According to the application, the range of connectivity required between the sensor nodes of IoT network differs. Most IoT applications demand short-range connectivity and are attached to NFC (Near Field Communication), Bluetooth, Zigbee, Z-Wave or BLE (Bluetooth Low Energy) protocols where as some others require connectivity over a few kilometers. The medium range applications employ connectivity options like Wi-Fi, WLAN (Wireless Local Area Network),

Received 12 April 2022, Accepted 30 June 2022, Scheduled 22 July 2022

* Corresponding author: Rashmi Roges (rashmiroges2019@gmail.com).

[1] Lovely Professional University, Phagwara, Punjab, India. [2] Department of Electronics and Communication Engineering, Bhagwan Parshuram Institute of Technology, New Delhi, India. [3] Division of Research and Innovation, Uttaranchal University, Dehradun, Uttarakhand, India.

NB-IoT (Narrow-Band IoT), LoRa (Long Range) Networks, etc. Long range applications are usually covered by LPWAN (Low Power Wide Area Network) technology, Cellular, GSM (Global Systems for Mobile Communication), SIGFOX, etc. which emphasize the coverage over longer distances. Figure 1 gives a clear picture of some common communication protocols employed to achieve different ranges of connectivity.

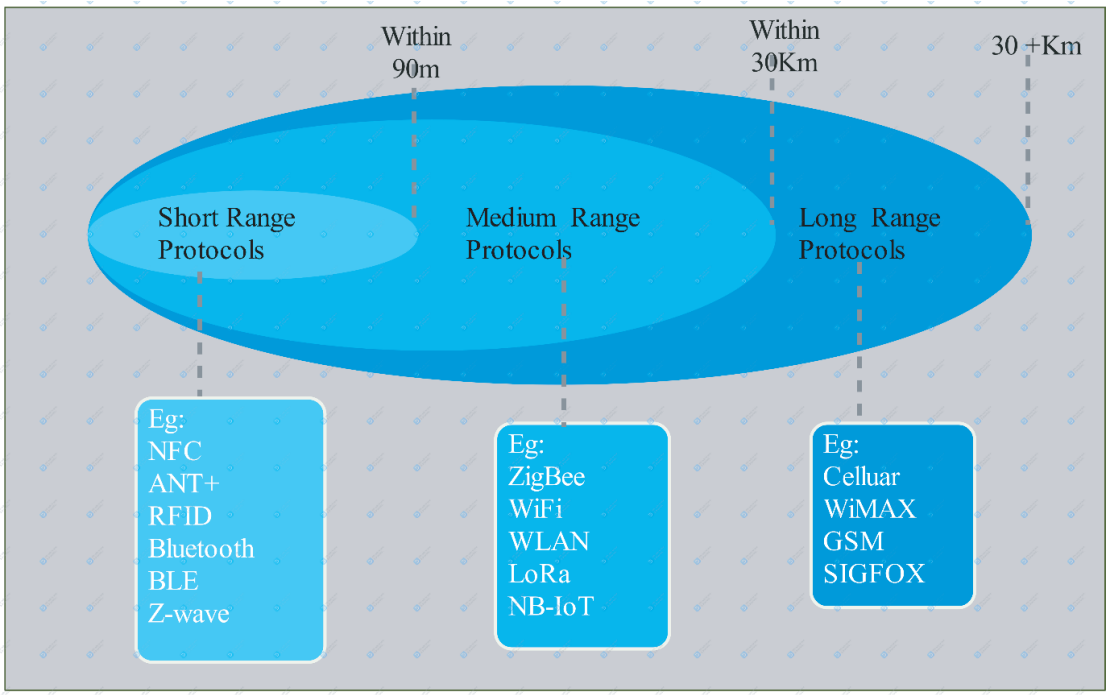

Figure 1. Communication Protocols for different range of connectivity.

The integration capability, i.e., the incorporation of different communication bands within a single system, is an inevitable demand of the present-day wireless systems to achieve multiple application support on a device. Antennas with simple design and multiband operation capability are in high demand for modern wireless systems [8]. IoT antennas are preferred to be small, power efficient, and cost-effective while supporting operations in various communication bands like IEEE 802.11 a/b/g/n (WLAN), GSMband, LTE(Long Term Evolution) band, and IEEE 802.16 WiMAX (World Wide Interoperability for Microwave Access) simultaneously which greatly supports efficient medium range applications [9–14]. The antenna proposed in this paper has a wide band, covering WLAN and WiMAX communication bands. With simple installation and comparatively wider coverage area, WiMAX systems have an upper hand than other technologies. WiMAX technology, which has been in the shadow of LTE, can become an alternative potential technology for IoT [15]. The key features of WLAN and WiMAX are summarized in Table 1.

There are both SISO (Single Input Single Output) and MIMO mode antennas designed for IoT applications. A broadband flexible antenna is proposed with a CPW (Co-Planar Waveguide) feed with an operating bandwidth between 0.856 GHz and 2.513 GHz and a radiation efficiency of 75% [16]. Another L-shaped planar antenna with 4 inputs was designed to operate at 3.5 GHz, 12.5 GHz, and 17 GHz [17]. In [15], an inverted six shaped antenna operating between 3.2 and 3.4 GHz is proposed with a maximum gain of 6 dBi. A triband MIMO antenna is also seen in literature with polarization diversity and a maximum ECC of 0.0471 [18]. A two-slot array antenna is proposed for 5.8 GHz frequency with an efficiency of 94% for ISM (Industrial Scientific and Medical) and Wi-Fi band IoT applications [19].

The proposed antenna is smaller in size than the other antennas and has an operational range in sub-6 GHz spectrum between 2 GHz and 4 GHz including the WiMAX and WLAN operational bands thus enabling the proposed system for WiMAX and WLAN bands of IoT applications.

Table 1. Key features of WLAN and WiMAX systems.

Specification	WiMAX	WLAN
Standard	IEEE 802.16 d/e	IEEE 802.11b
Data Rate	70 Mbps	1–54 Mbps
Coverage distance	50 km	Around 100 m
Operating Frequency	2.3 GHz, 2.5 GHz and 3.5 GHz	2.4 GHz and 5.8 GHz
Channel Bandwidth	1.25 to 20 MHz	25 MHz
Applications	Broadband Connectivity, USB Dongles, Metropolitan Area Networks	Automation of substations, Control and Monitoring of sensor nodes

Today's wireless systems demand ultra-high data rates for unhindered, low latency services like high quality video streaming while being expected to assist low data rates, low latency, and secure connections between small IoT sensor nodes [23]. MIMO technology promises better channel capacity and coverage along with high data rates without any extra bandwidth [24]. A compact MIMO antenna system, which can support multiple communication technology will be highly advantageous to fulfill the current demands that aids voice and data communication at high data rates while supporting the real time communication of a huge number of small IoT nodes.

The scope of log-periodic antenna for IoT applications has never been exploited so far. The novelty of the proposed work is in terms of the application and not design. This article presents an antenna for IoT applications which require stable gain and particular bandwidth because Log-periodic antennas were employed for HF/UHF/VHF and television reception applications so far. A compact two port MIMO antenna of size 15 mm × 17 mm × 1.6 mm is proposed for medium and long-range connectivity of IoT nodes through WiMAX and WLAN technologies. The antenna is built on a low-cost FR-4 substrate. Defected Ground Structure (DGS) technique is employed to enhance the bandwidth and shift the working frequency to the desired range of operation while suppressing the mutual coupling between the two individual radiating elements.

2. ANTENNA DESIGN AND ANALYSIS

The schematics of the top and bottom views of the proposed antenna is as shown in Figure 2. The antenna configuration is similar to the single sided planar trapezoidal toothed log periodic antenna. The pattern is unidirectional towards the apex of the cone formed by the two arms. The peculiar thing about antenna configuration is that the fields on the conductors attenuate very sharply with distance. This concludes that perhaps there is a strong current concentration at or near the edges of conductors. This type of antenna configuration generally provides linear polarization. Since the edges are made linear (instead of curved), it results in more convenient fabrication geometry with basically no loss in operation performance. The antenna is fed by a microstrip feedline as shown in Figure 2(a).

A MIMO antenna system is known to provide better signal strength and would be useful to cover more range than a single element antenna. MIMO system utilizes the reflected and bounced RF signal to constructively improve the system performance. MIMO can also provide higher throughput, which in turn can attain better quality of received RF signal in a network. Antennas, when being used for IoT applications, need to be compact for easy installation. However, it is challenging to implement multiple radiating antenna elements in the common substrate as the closely placed elements will have a tendency to 'talk to each other', and that is the basic cause of mutual coupling.

A single element structure is displayed in Figure 2(a) whereas a two element MIMO structure is designed on a common ground plane to form Ant I. The schematic view of design evolution steps of the final antenna is displayed in Figure 2(b). Ant I offers an impedance bandwidth of 2.94 GHz without embedding any DGS. The simulated and measured S_{11} for Ant I are shown in Figure 3(a).

Embedding a defect in the ground plane has been seen to improve the performance parameters of

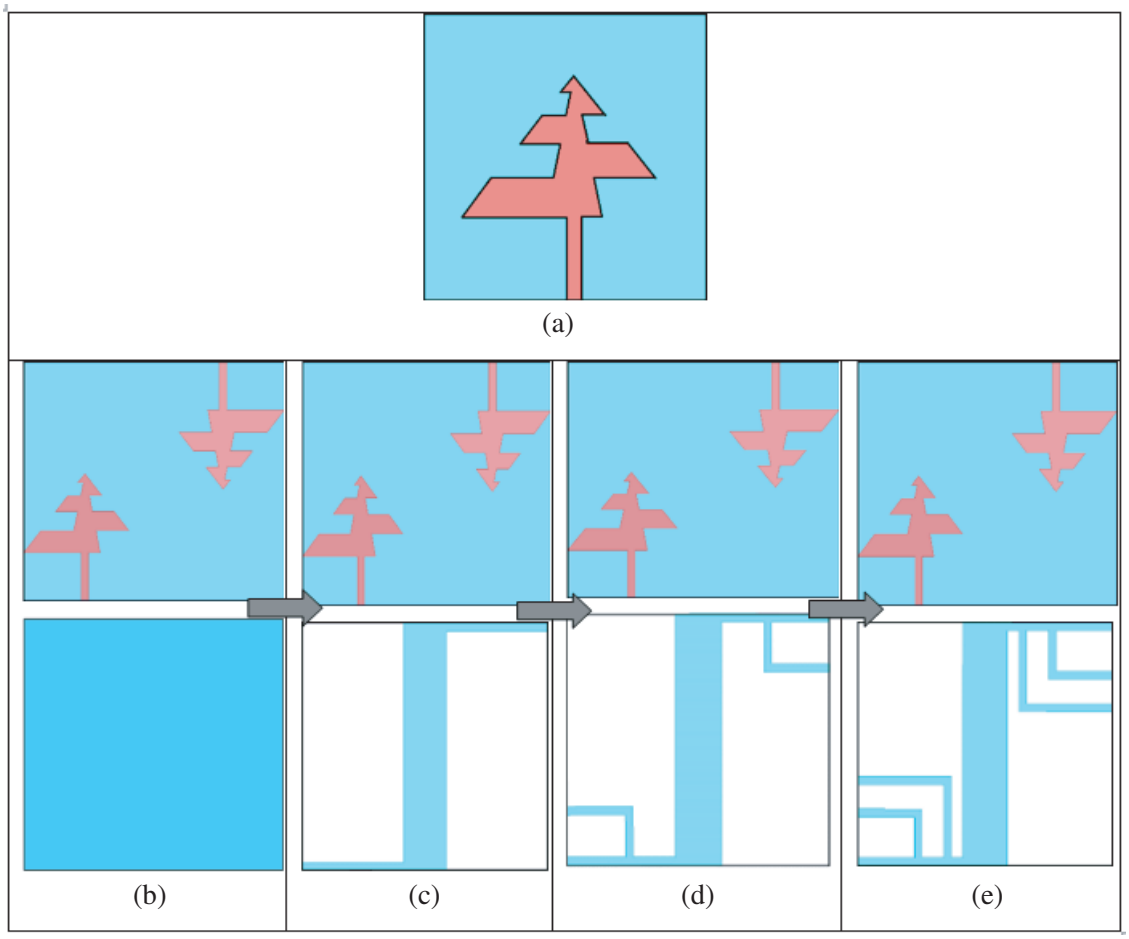

Figure 2. Schematic of the proposed antenna. (a) Single element, (b) Ant I, (c) Ant II, (d) Ant III, (e) Ant IV.

the antenna system in many a case. This technique is widely used and is called DGS (Defected Ground Structure). In the design methodology, the ground plane of Ant I is altered by adding two rectangular slots of size 14.5 mm × 7 mm to form Ant II. The addition of DGS alters the current distribution in Ant I ground plane and causes a variation in effective capacitance and inductance of the system. This enables to obtain an impedance bandwidth below −10 dB as shown in Figure 3(b) in Ant II. The top and bottom planes of Ant II are shown in Figure 2(c). Ant II offers an impedance bandwidth of 2 GHz ranging from 2.69 GHz to 4.69 GHz as shown in Figure 3(b). The mutual coupling between the two ports of Ant II was found below −20 dB. An L-shaped rectangular slit of $L_{12} \times W_{14}$ and width 0.3 mm is further added to the ground plane of Ant II to form Ant III. The schematic of top and bottom views of Ant III is shown in Figure 2(d). Ant III offers the same bandwidth as Ant II but ranging from 2.48 GHz to 4.47 GHz with a further reduced mutual coupling below −24 dB. The simulated and measured S parameters for Ant III are as shown in Figure 3(c). Another rectangular slit of $L_{10} \times W_{16}$ with a width of 0.5 mm is added to Ant III to design Ant IV. Ant IV again offers a proper shifting in the band and is shifted towards the left, now ranging between 2.06 GHz and 4.04 GHz with an isolation of more than −30 dB throughout the bandwidth. The front and back views of Ant IV are given in Figure 2(e). The return loss for Ant IV is as shown in Figure 3(d).

Figures 4(a) and 4(b) show the dimensions of the proposed antenna and its ground plane with all the values of the variables listed in Table 2.

3. RESULTS AND DISCUSSIONS

The two port MIMO antenna was designed and fabricated on a low-cost FR4 substrate of dimension $L \times W$ with a thickness of 1.6 mm as described in Table 2. FR4 (Flame Retardant), being one of the most commonly used materials for PCBs, is known for its brittleness, insulation between layers, maintenance of signal integrity, and minimizing interference. It has a dielectric constant of 4.4 with a loss tangent of 0.02. The antenna was fabricated for experimental measurement of parameters using Network Analyzer, Spectrum Analyzer, and Anechoic Chamber. Sub-Miniature version A (SMA) connectors are used as co-axial RF connectors to connect the ports to the analyzer. The SMA connector has an impedance of

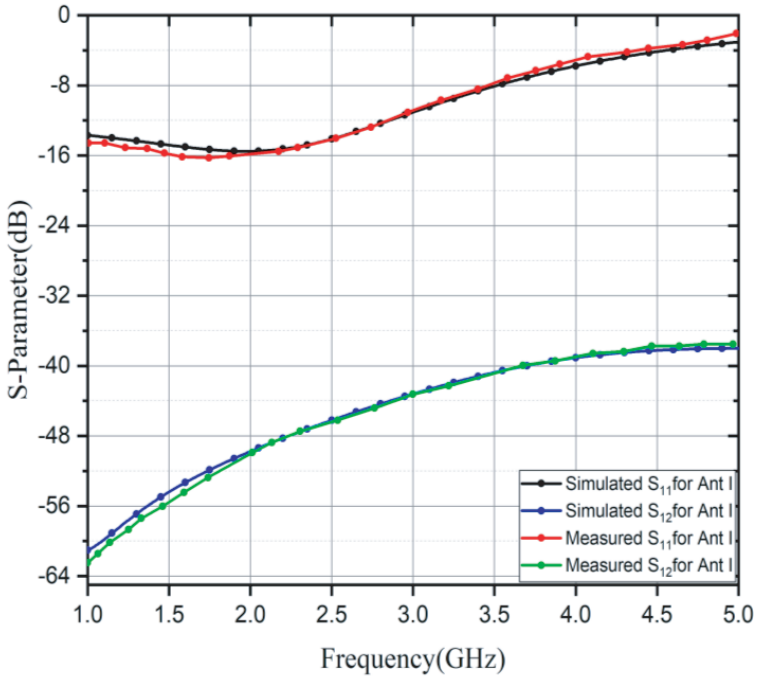

(a)

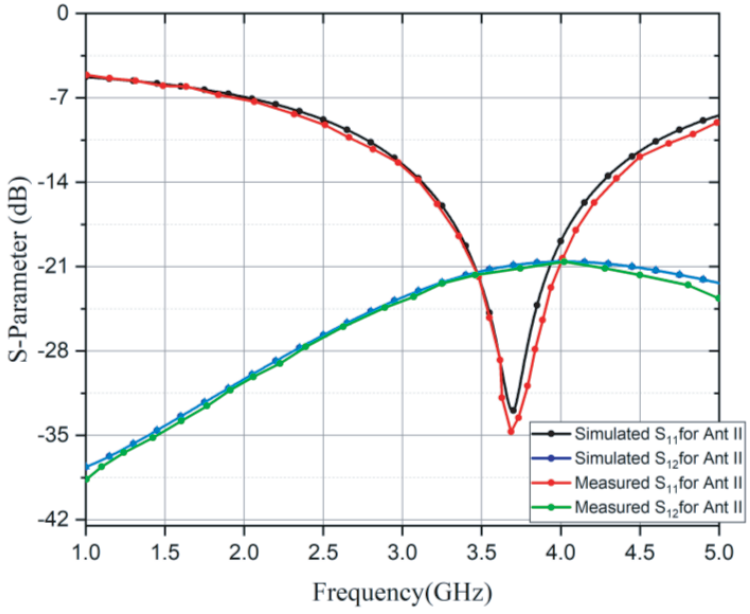

(b)

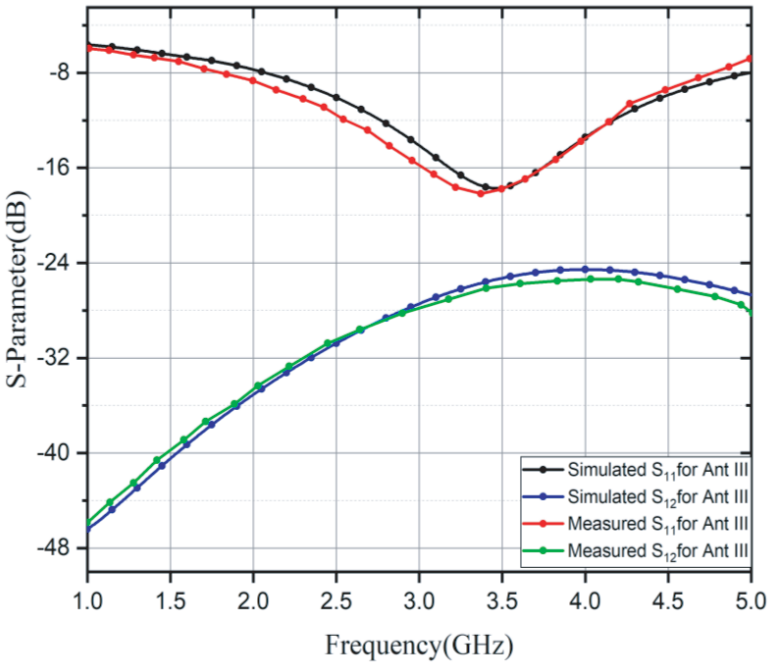

(c)

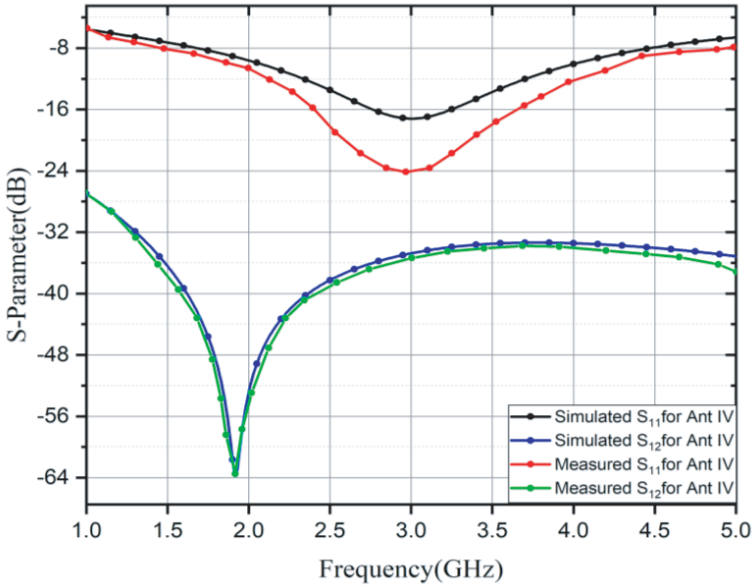

(d)

Figure 3. Simulated and measured S-parameter variations with frequency for all stages. (a) Ant I, (b) Ant II, (c) Ant III, and (d) Ant IV.

50 Ω. Figure 5(a) shows the fabricated prototypes of the designed antenna. The experimental setup for the measurement is displayed in Figure 5(b).

3.1. Parametric Analysis

A bunch of parametric study was done on the ground plane to optimize the DGS of the design and finalize the proposed final antenna structure. A rectangular slot of $l \times w$, as shown in Figures 6(a)

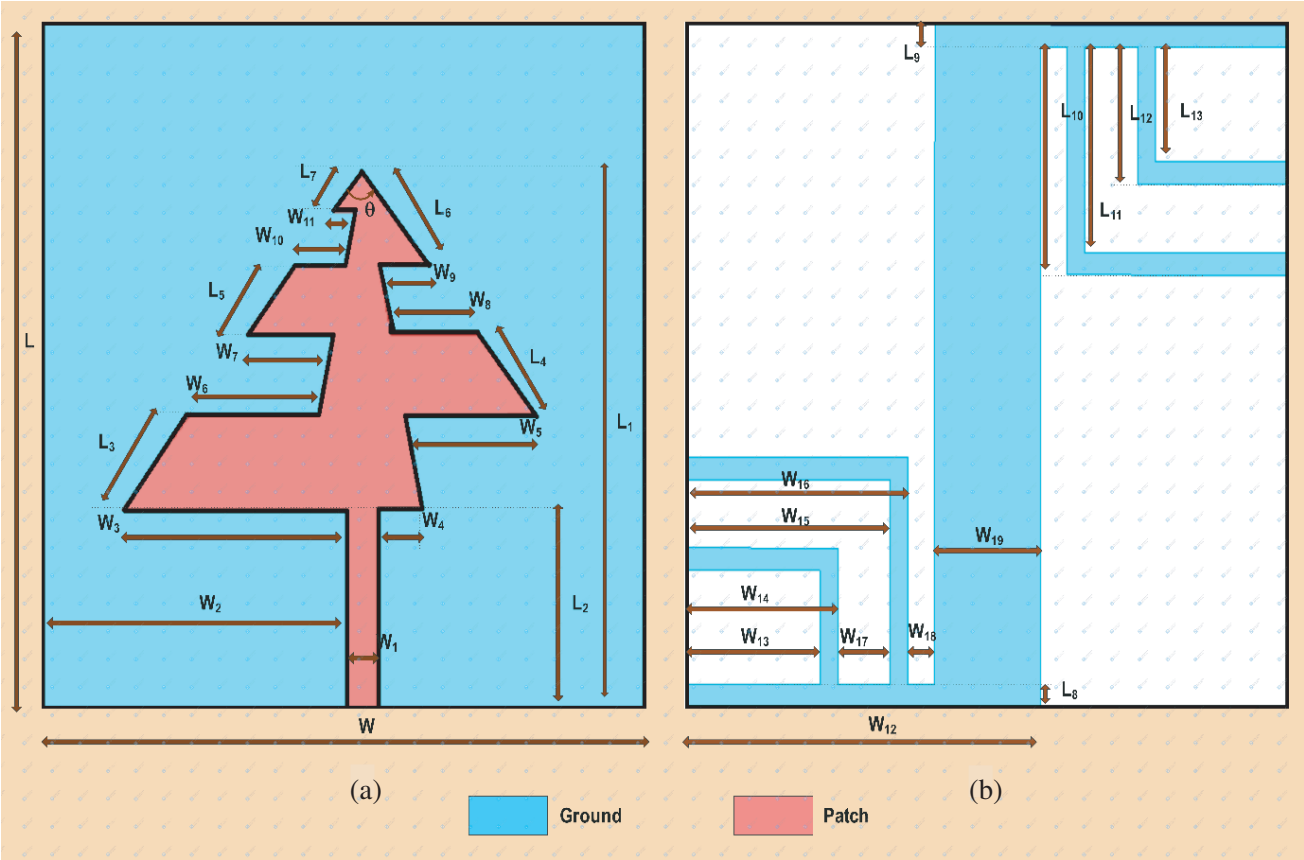

Figure 4. Dimensions for the proposed Ant IV. (a) Radiating patch. (b) Ground plane.

and 6(c), was cut on the ground plane. The return loss of $-31.6\,\text{dB}$ was achieved for $l = 14.5\,\text{mm}$ as shown in Figure 6(b). Similarly, the width w of the rectangular slot on the ground was also studied parametrically to observe its effect on the return loss. The bandwidth seemed almost unaffected by width variations, but the return loss could be improved to $-35.49\,\text{dB}$ at $w = 7\,\text{mm}$ as shown in Figure 6(d). The rectangular slot was thus optimized to be $14.5\,\text{mm} \times 7\,\text{mm}$ from either side ends of the ground plane.

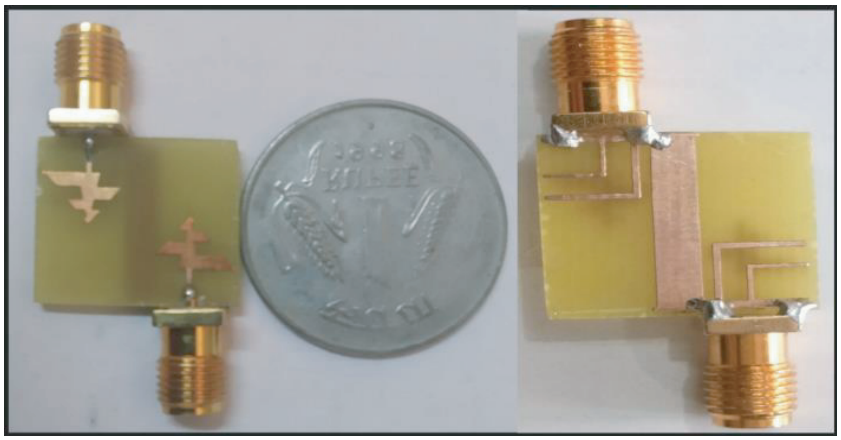

(a)

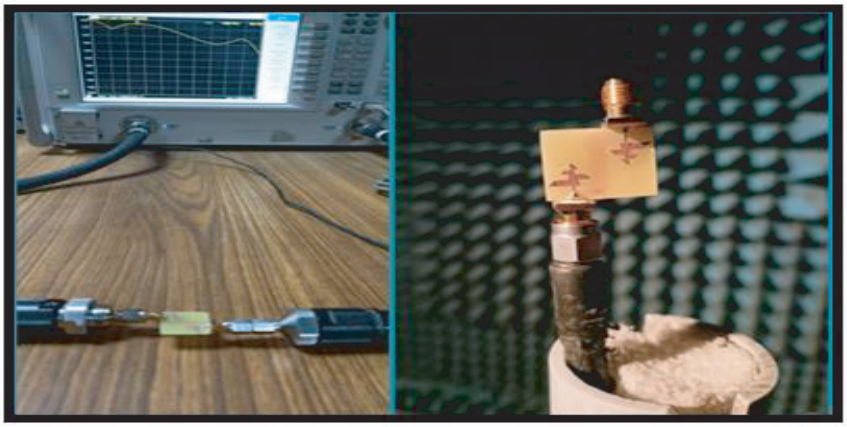

(b)

Figure 5. (a) Fabricated prototypes of the proposed antenna. (b) Measurement setup for the proposed antenna.

Two L-shaped slits were then attached further to the DGS by which the impedance bandwidth shifted, and the mutual coupling was improved. The inner slit attached shifted the bandwidth from (2.69 GHz–4.69 GHz) to (2.48 GHz to 4.47 GHz) while improving the isolation to below −24 dB. Parametric analysis was applied to the width w of this L-shaped rectangular slit as shown in Figure 7(a), and the best return loss of −19.82 dB was attained for a width of $w = 0.3$ mm as shown in Figure 7(b).

The second, bigger L-shaped slit was found to further shift the impedance bandwidth to (2.06 GHz–4.04 GHz) and further improved the isolation to below −30 dB. A parametric study on the width of this L-shaped slit showed that the return loss was maximized at the width $w = 0.5$ mm. Figure 7(c) and Figure 7(d) show the details of the parametric analysis done on the width of the L-shaped slit and the corresponding return loss plot, respectively.

The power received or transmitted in a specific direction measures the gain of an antenna, and it' i measured by comparing the power radiated in a specific direction by the antenna to the peak radiation of an isotropic source. DGS has a significant effect on the gain of microstrip antenna. We know that for a microstrip antenna, there is a current redistribution when DGS is used on ground plane which causes an interference between waves, and this current redistribution opens an opportunity in gain enhancement for the antenna. Figure 8 shows the measured and simulated variations in gain with respect to frequency for all stages of the proposed design. Over the range of operating frequency, the gain of the final design varies from 0.96 dB to 2.9 dB with a maximum gain of 2.9 dB at 2.56 GHz. The

Table 2. Parameter specifications for proposed antenna (Ant IV).

Dimensions of the Patch				**Dimensions of the Ground Plane**			
W	17 mm	L	15 mm	W_{12}	10.0 mm	L_8	0.50 mm
W_1	0.5 mm	L_1	7.5 mm	W_{13}	3.75 mm	L_9	0.50 mm
W_2	3.75 mm	L_2	2.5 mm	W_{14}	4.0 mm	L_{10}	5.0 mm
W_3	3.75 mm	L_3	1.792 mm	W_{15}	5.75 mm	L_{11}	4.50 mm
W_4	0.75 mm	L_4	1.536 mm	W_{16}	6.25 mm	L_{12}	3.0 mm
W_5	2.14 mm	L_5	1.280 mm	W_{17}	1.70 mm	L_{13}	2.75 mm
W_6	2.15 mm	L_6	1.792 mm	W_{18}	0.75 mm		
W_7	1.44 mm	L_7	0.768 mm	W_{19}	3.0 mm		
W_{10}	0.84 mm						
W_{11}	0.38 mm						

gain stays positive over the entire operating range of 2 GHz to 4 GHz frequency. Radiation efficiency is another parameter that measures the effectiveness of an antenna by measuring the power radiated by the antenna to the power received by the antenna. The efficiency of the proposed antenna is almost constant over the frequencies from 2 GHz to 4 GHz, and the measured and simulated efficiencies are in good agreement with each other. Figure 9 shows that the radiation efficiency of the designed Ant IV is about 92.8%.

The *E*- and *H*-plane normalized radiation patterns for the proposed antenna are shown in Figures 10(a) and 10(b). The radiation patterns for the transmitting and receiving antennas in line (Co-polarization) and the radiation patterns for the transmitting and receiving antennas being orthogonal (Cross-polarization) for both *E*-plane and *H*-plane are given in Figures 11(a) and 11(b), respectively.

3.2. MIMO Antenna System Performance

A MIMO antenna system employs more than one antenna at the transmitter side, receiver side, or both transmitter and receiver, to achieve better throughput and data rates. MIMO system helps to ensure an optimal wireless performance when single antenna technology evolves to its limits in terms of parameters like channel capacity and transmitted power limitations. Use of multiple antennas is proved to be the key technology for performance enhancements in such scenarios. The channel fading and multipath

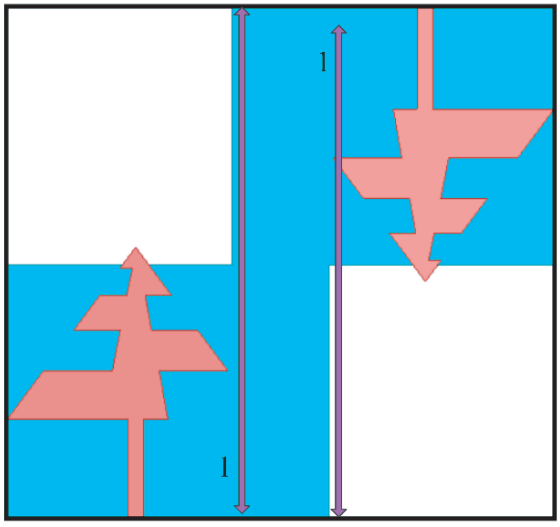

(a)

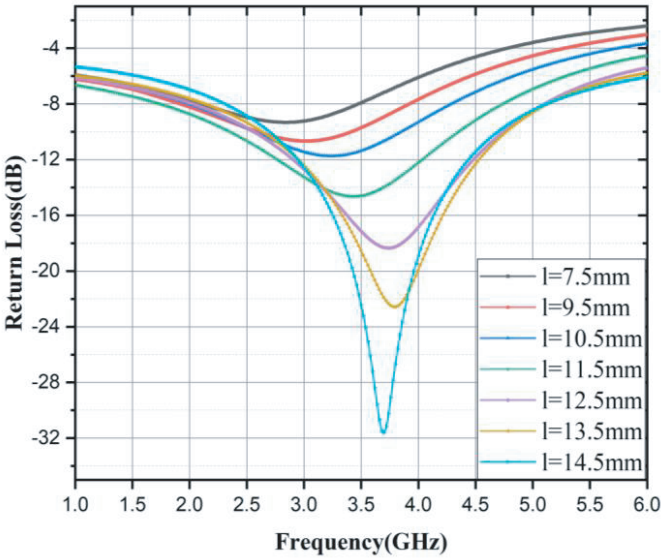

(b)

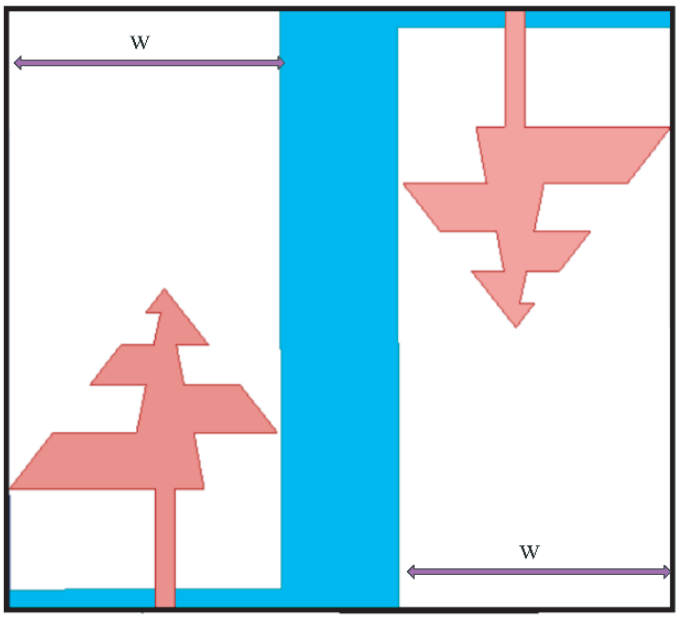

(c)

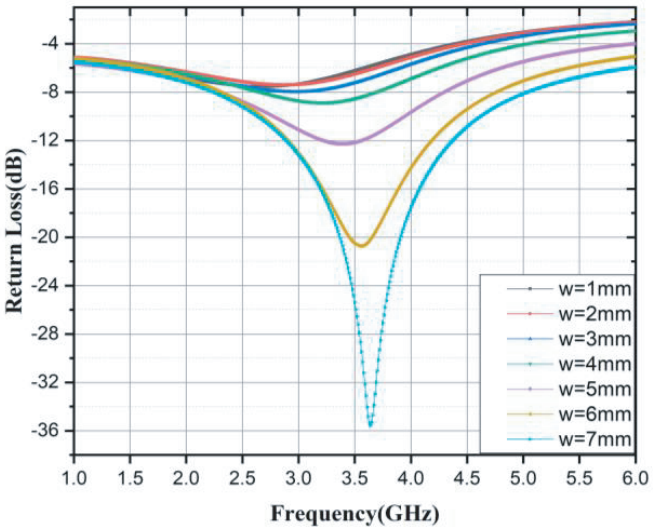

(d)

Figure 6. Parametric study done on the length and width of the rectangular slot etched in the ground plane. (a) Length variations of the slot. (b) Parametric analysis result on various lengths varying from 7.5 mm to 14.5 mm and maximum return loss at $l = 14.5$ mm. (c) Width variations of the slot. (d) Parametric analysis result on various lengths varying from 1 mm to 7 mm depicting maximum return loss at $w = 7$ mm.

propagation which arises while the signal travels through the channel with obstacles like buildings and trees can be compensated by using multiple antennas to send the same signal simultaneously. Spatial Multiplexing and Diversity Gain are two key factors which would decide the system performance as per the demands of a specific application. When a MIMO system offers various advantages, it also presents some challenges. The major challenge is to isolate the performance of the individual antennas when they are made to share the same substrate. The isolation or mutual coupling between the elements of a MIMO system is evaluated to access the performance of the antenna system designed. A MIMO system is evaluated by the parameters like ECC, DG, and TARC.

3.2.1. Suppression of Mutual Coupling

MIMO systems are an arrangement of multiple antenna elements, identical or non-identical, on the same substrate to obtain better channel capacity without any additional increase in the transmitting power. Mutual coupling defines the energy absorbed by an adjacent antenna when another antenna is radiating. Mutual coupling has a tendency to change the radiation pattern, reflection coefficient, and input impedance of the MIMO antennas. The periodic L-shaped defected ground structure unit has been placed between antenna radiating elements to reduce mutual coupling. It interrupts the EM far field significantly and induces the current between patch elements. The coupling between two microstrip antenna elements is the function of relative alignment due to two side by side radiating elements. Without DGS unit large surface current is induced on the coupled antenna elements resulting in higher mutual coupling. However, in the presence of etched DGS surface induced current is significantly reduced due to its confinement within restricted substrate area. Figure 12 shows the comparison of the isolation levels in all the stages of the antenna design. The DGS has improved the isolation between the elements.

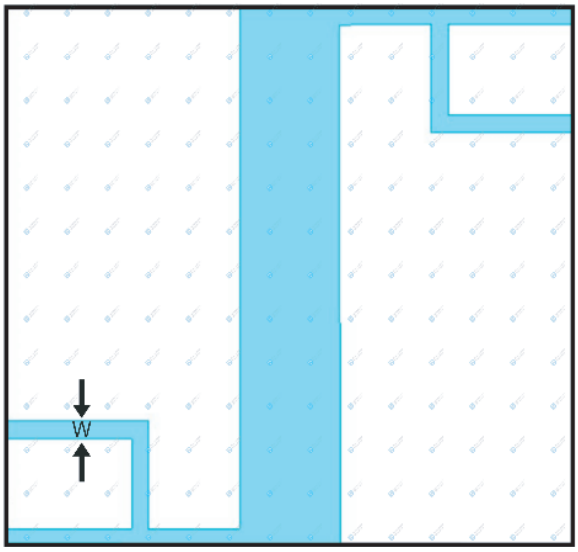

(a)

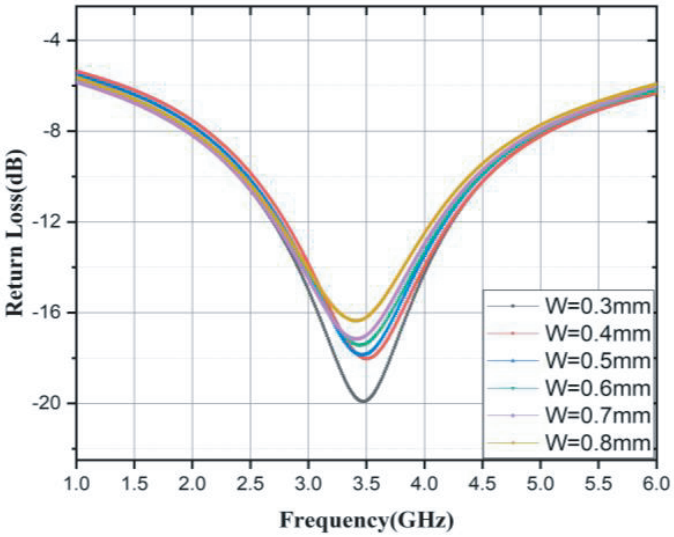

(b)

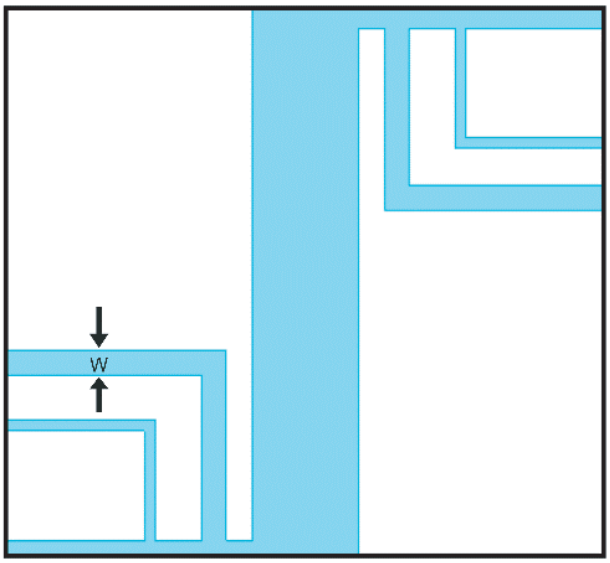

(c)

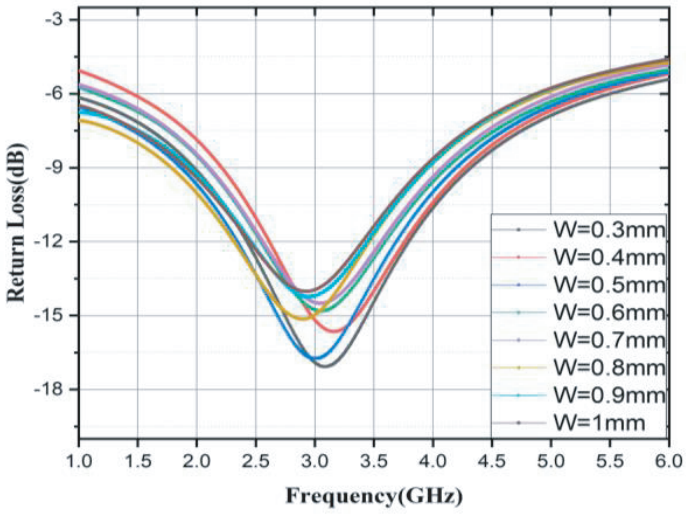

(d)

Figure 7. Parametric study done on the width of the rectangular L-shaped slit etched in the ground plane. (a) Width variations of the inner slit. (b) Parametric analysis result on various widths varying from 0.3 mm to 0.8 mm showing maximum return loss when $w = 0.3$ mm. (c) Width variations of second slit. (d) Parametric analysis result on various widths varying from 0.3 mm to 1 mm showing maximum return loss at $w = 0.5$ mm.

3.2.2. ECC (Envelope Correlation Coefficient)

ECC is one of the major performance evaluators of a MIMO antenna which measures the level of decoupling between the individual antenna elements and the amount of correlation between the elements. Ideally, there should not exist any interference between the radiations of the co-existing antenna elements, and the value of ECC should be zero. Nevertheless, for practical MIMO antenna systems, an ECC value of below 0.5 is acceptable. ECC of a MIMO antenna with respect to the radiated fields is theoretically evaluated by (1).

$$ECC = \frac{|S_{11} * S_{12} + S_{21} * S_{22}|^2}{\left(1 - |S_{11}|^2 - |S_{21}|^2\right)\left(1 - |S_{22}|^2 - |S_{12}|^2\right)} \tag{1}$$

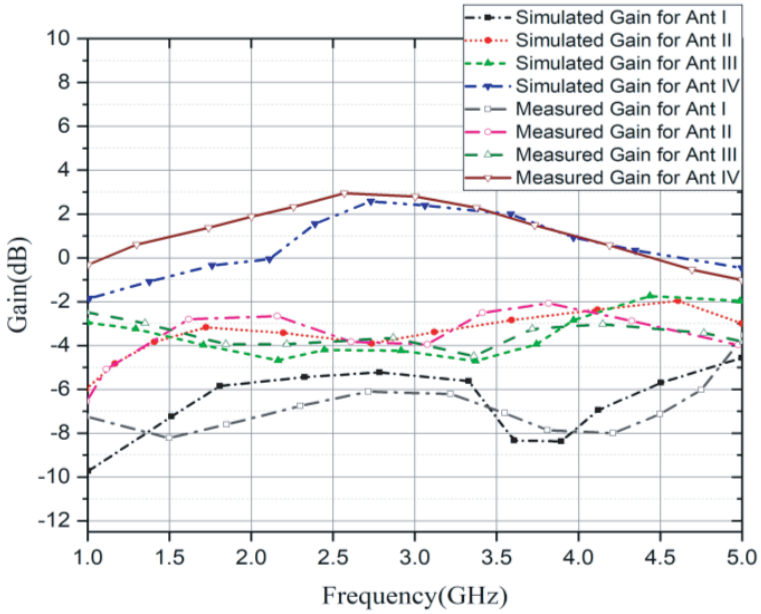

Figure 8. Simulated and measured gain variations for all stages of the proposed antenna (Ant IV).

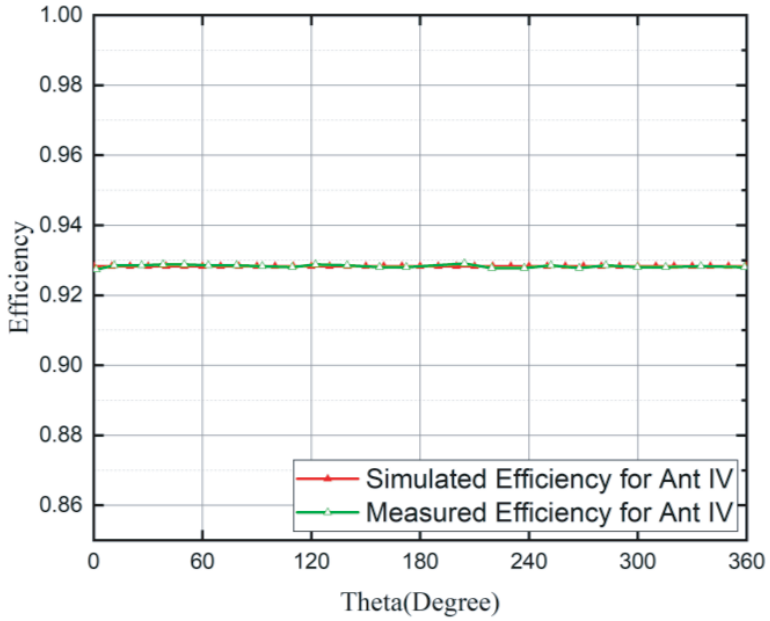

Figure 9. Simulated and measured efficiencies for the proposed antenna (Ant IV).

The ECC of the proposed antenna is shown in Figure 13. It is clearly seen that, for the operating range of the proposed MIMO system, which is 2.01 GHz to 4.04 GHz, the ECC value is well below 0.0002. The simulated and measured ECCs for Ant IV are shown in Figure 13.

3.2.3. DG (Diversity Gain)

Diversity gain is another parameter calculated for an antenna system with more than one radiating element. The multipath signal reflection, generally considered as a challenge, is exploited in a MIMO

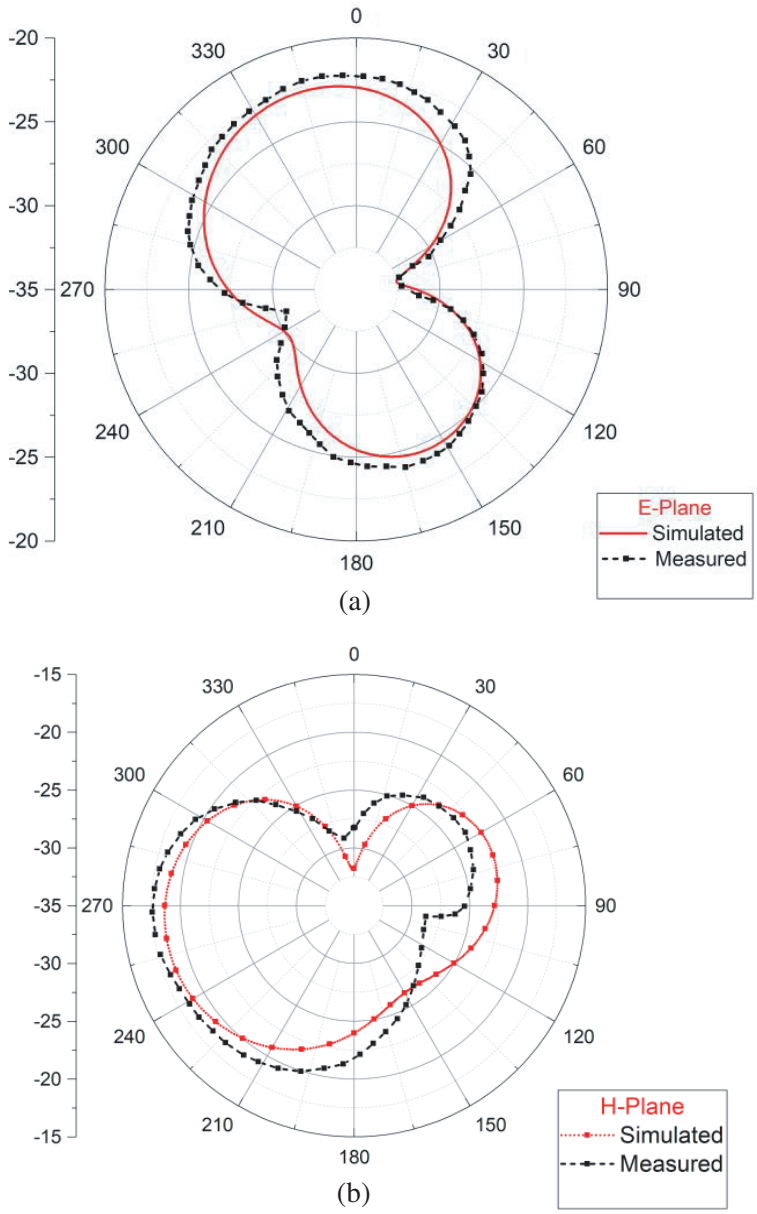

Figure 10. Simulated and Measured Radiation patters for the proposed antenna (Ant_IV). (a) E-plane at 3 GHz. (b) H-plane at 3 GHz.

system. The signal received from multiple paths provides diversity gain, and this helps the recovery of data by an intelligent receiver. The value of this parameter is desired around 10 and above 9.95. The equation for theoretical calculation of DG is given in (2). The DG for the proposed MIMO antenna is above 9.99.

$$DG = 10\sqrt{1 - ECC} \tag{2}$$

3.2.4. TARC (Total Active Reflection Coefficient)

In a MIMO system, multiple antennas work simultaneously, and it is fairly obvious that the elements impinge on each other. The S-parameters alone will not be sufficient to characterize a MIMO system

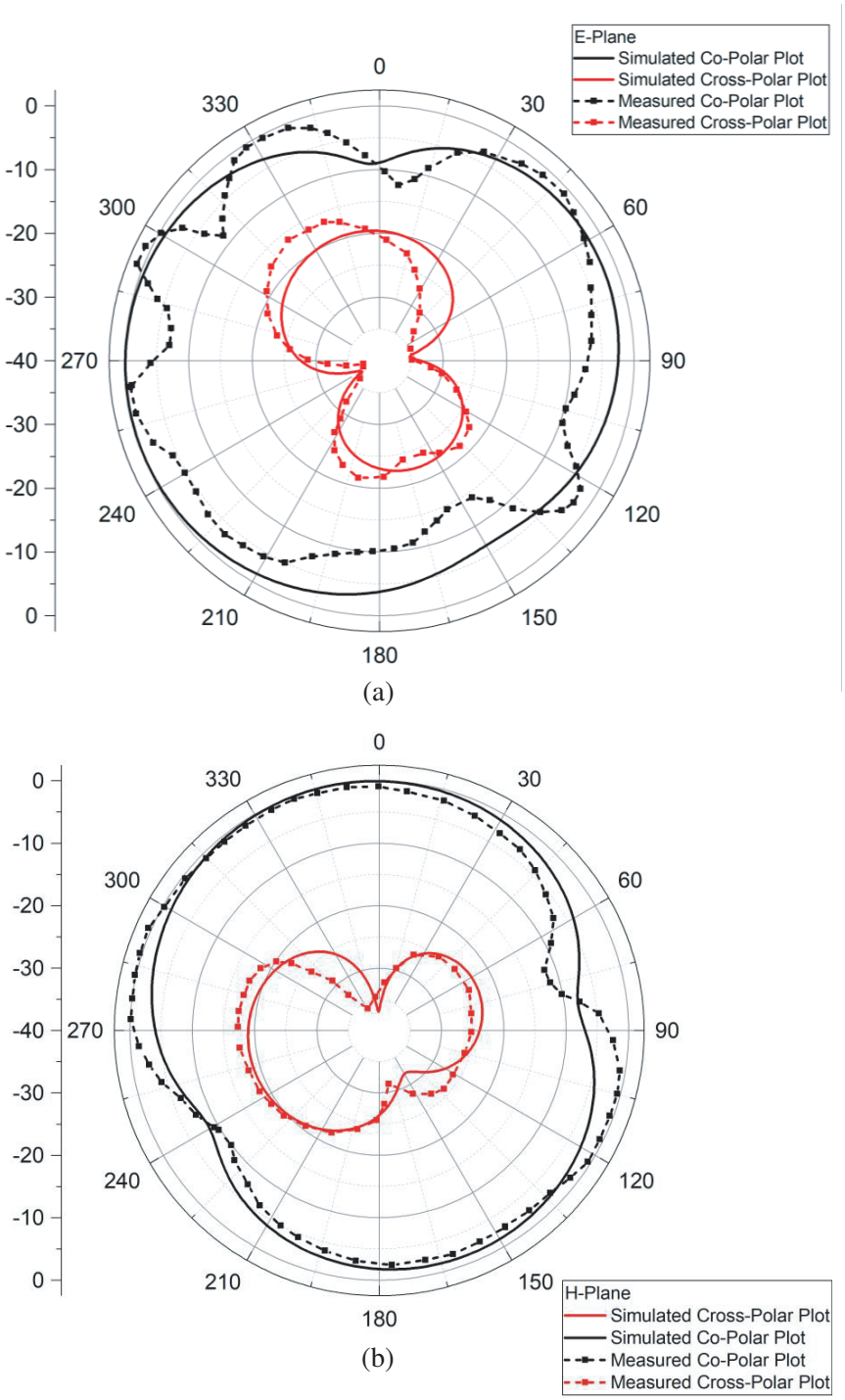

Figure 11. Simulated and measured co-polarization and cross-polarization radiation patterns for the proposed antenna (Ant_IV). (a) E-plane at 3 GHz. (b) H-plane at 3 GHz.

as the parameters like bandwidth, performing efficiency, and the gain of the system will be deeply influenced by the interaction between the element radiators. Another parameter so defined for a MIMO antenna is TARC which is the relation between the reflected power and the total power incident on the

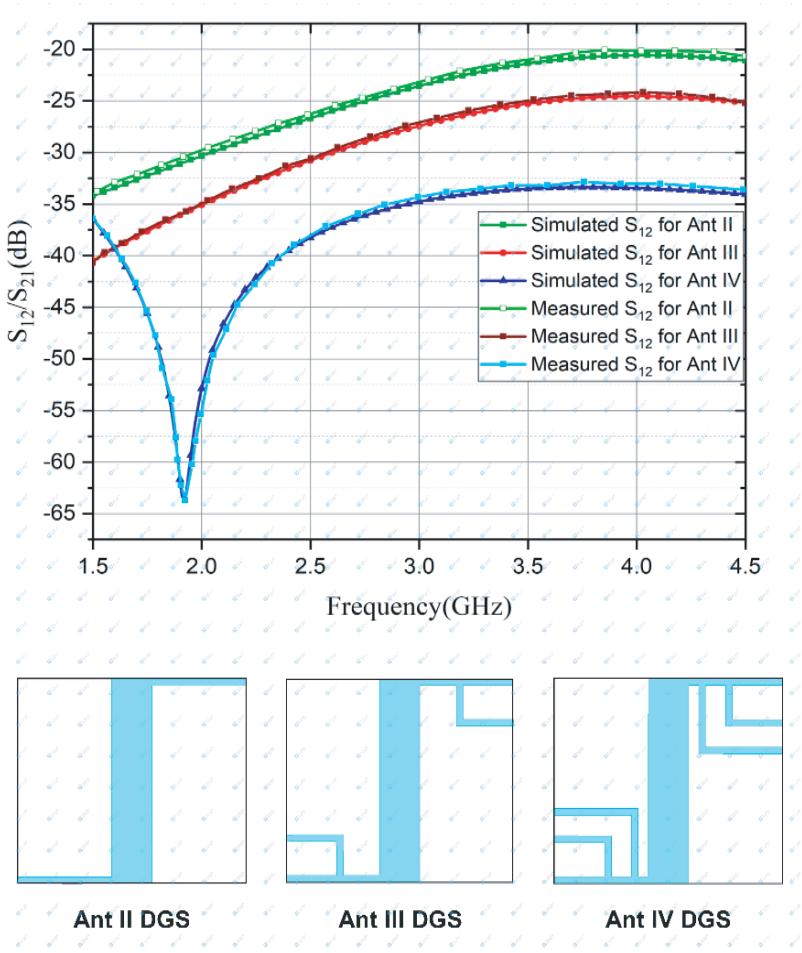

Figure 12. Simulated and measured isolations between the two elements in Ant II, Ant III, and Ant IV.

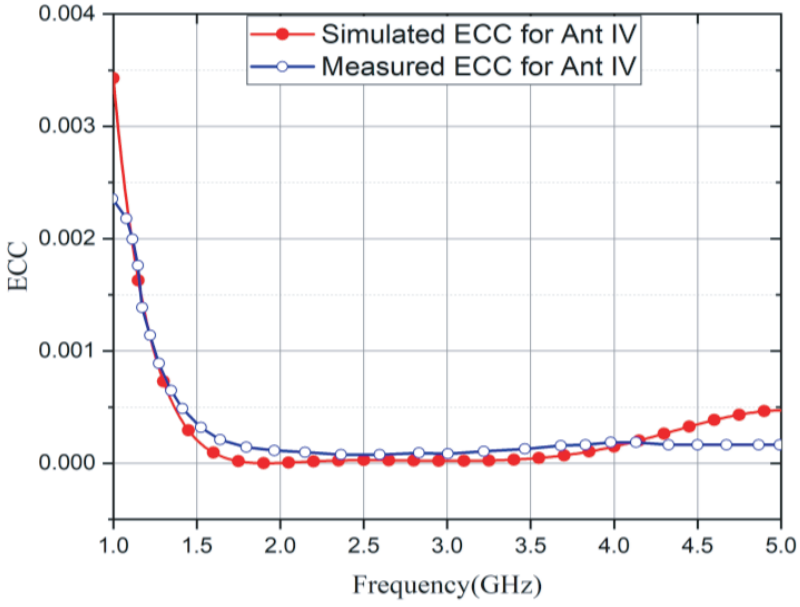

Figure 13. Simulated and measured ECCs for the proposed antenna (Ant IV).

system. TARC for a two port MIMO antenna is calculated by the formula given in (3).

$$TARC = \sqrt{\frac{(S_{11} + S_{12})^2 + (S_{21} + S_{22})^2}{2}} \tag{3}$$

The simulated and measured values for TARC and DG for Ant IV are given in Figure 14.

Table 3. Comparison of the proposed antenna with other relevant work in the literature.

Ref.	Size	Operating Bandwidth /Frequency	Number of Ports	Gain/Peak Gain	Efficiency	Isolation Technique and Isolation	Proposed Application	ECC
[8]	140 × 120	2.34–2.56	4	2 dBi	> 79%	Use of Parasitic element < −14 dB	Wi-Fi Applications	< 0.01
[9]	56 mm ×56 mm ×0.5 mm	(1.3–40) GHz with three notch bands 2.4 GHz, 5.5 GHz, and 7.5 GHz	4	7 dBi	Not Given	Orientation of the elements. < −22 dB	IoT Applications	< 0.03
[10]	92 mm ×121.2 mm ×2 mm	3.5 GHz 12.5 GHz and 17 GHz	4	> 6.34 dB	> 81%	Complementary Modified Split Ring Resonator (CMSRR) in the ground. < −18 dB	4G/5G and IoT Applications	< 0.08
[11]	33 mm ×57.25 mm ×1.6 mm	1.89 GHz and 2.45 GHz	2	> 0.758 dB	> 72.12%	Orientation of the elements < −14.2 dB	IoT Applications	< 0.0471
[12]	140 × 120	2.25–2.7	4	5.33–6.97 dBi	> 57%	Use of Parasitic element < −14 dB	Wi-Fi and LTE Applications	< 0.2
[15]	27 × 21	(5.19–5.41) GHz and ((7.30–7.66) GHz	2	> 9.38 dB	79.8%	Orthogonal Polarization < −22.5 dB	WLAN and X-Band Satellite Applications	< 0.4
[16]	55 × 65	2.4–2.5	2	4.5 dBi at 2.45 GHz and 5.3 dBi at 5.25 GHz	60–65%	Use of decoupling network < −15	LTE and WiMAX Applications	< 0.15
[17]	50 × 61.5	2.35–2.5	3	NA	51–82%	Use of decoupling network < −20	Electrically small and symmetric platforms, such as cars, and ships.	< 0.04
[18]	32 × 28	(2.26–2.58) Hz and (2.58–6.88) GHz	2	5.2 dB	Not Mentioned	Double Split Ring Resonator < −24 dB	Bluetooth, WLAN and WiMAX Applications	< 0.05
[19]	60 × 55	(2.3–23) GHz	4	4.5 dBi	(60–90)%	A stub in the ground plane along with orthogonal placement of the component elements. < −20 dB	IoT and High speed applications	< 0.002
[20]	120 × 110	(1.97–3.317) GHz	2	5.4 dB	92%	Use of double slit complementary split ring resonator. < −15 dB	WiMAX Applications	< 0.5
[21]	25 × 25	(0.66–1.06) GHz and (1.68–2.88) GHz	2	−0.2–3.5 dBi	(38–85)%	Using defected ground and grounded branching. < −13.5	Wireless terminal applications	< 0.15
[22]	34 × 34	(0.7–3.8) GHz and (3.3–7) GHz	2	Not Mentioned	< 75%	Polarization Diversity. < −20 dB	Mobile handsets and IoT Applications	Not Mentioned
[23]	65 mm ×120 mm ×1.56 mm	(754–971) MHz, (1.65–1.83) GHz, (2–3.66) GHz, (3.9–4.1) GHz (4.8–5.5) GHz and (5.82–5.93) GHz	5	4.9 dBi	Not Given	Not Given	IoT Applications	< 0.5
[24]	54.98 mm ×76 mm ×1.6 mm	(2.1–4.0) GHz	4	2.83 dBi	> 82%	Use of Parasitic element and design of ground plane. < −12 dB	Human Interface Device and S-Band Applications	< 0.026
Proposed Antenna	**15 mm ×17 mm ×1.6 mm**	**(2.06 GHz −4.04 GHz)**	**2**	**2.9 dB**	**92.8%**	< −30 dB	**IoT Applications on WiMaX and WLAN frequencies**	< 0.0002

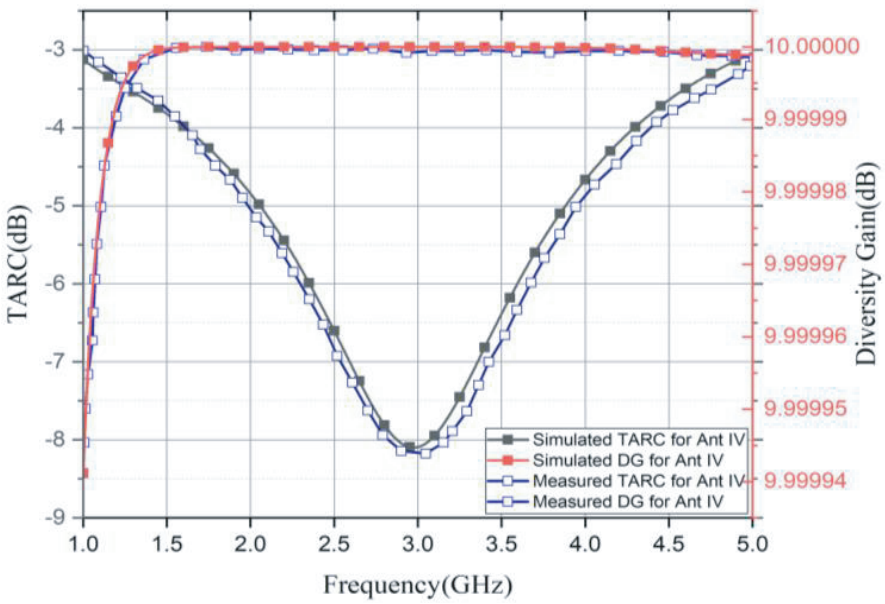

Figure 14. Simulated and Measured TARC and Diversity Gain for the proposed MIMO antenna.

A comparative analysis of Ant IV has been done with similar antennas present in the literature, and the study is summarized in Table 3. The proposed antenna (Ant IV) is highly compact and has excellent isolation between the two ports along with acceptable gain and good efficiency.

4. CONCLUSION

Communication module for IoT systems has been evolving rapidly over the last decade, and compact antennas with good performance are always pertinent. Log-Periodic antennas, which were widely used in TV reception and UHF/VHF applications, have been extended to IoT applications in this proposed paper. So the novelty of the proposed work is in terms of applications and not design. A two port MIMO antenna is designed, fabricated, and analyzed in this paper. The antenna designed matured through various stages, and the final stage of the designed antenna shows an impedance bandwidth of about 2 GHz ranging between 2.06 GHz and 4.04 GHz with good isolation of less than −30 dB. A maximum gain of 2.9 dB is achieved with an efficiency of 92.8%. The basic MIMO parameters as ECC (< 0.0002), DG (almost 10 dB, and TARC (less than −3 dB) are studied and are found to be in the acceptable range for a MIMO antenna system. The simulated and measured results are also found to be in good agreement with each other. This antenna, with a size as small as 15 mm × 17 mm, can be used in small IoT nodes which are employed in medium range IoT systems communicating using WiMaX and WLAN communication protocols.

REFERENCES

1. Lee, I. and K. Lee, "The Internet of Things (IoT): Applications, investments, and challenges for enterprises," *Business Horizons*, Vol. 58, No. 4, 431–440, 2015.
2. Roges, R. and P. K. Malik, "Planar and printed antennas for Internet of Things-enabled environment: Opportunities and challenges," *International Journal of Communication Systems*, e4940, 2021.
3. Kafle, V. P., Y. Fukushima, and H. Harai, "Internet of things standardization in ITU and prospective networking technologies," *IEEE Communications Magazine*, Vol. 54, No. 9, 43–49, 2016.

4. Agiwal, M., A. Roy, and N. Saxena, "Next generation 5G wireless networks: A comprehensive survey," *IEEE Communications Surveys & Tutorials*, Vol. 18, No. 3, 1617–1655, 2016.
5. Chettri, L. and R. Bera, "A comprehensive survey on Internet of Things (IoT) toward 5G wireless systems," *IEEE Internet of Things Journal*, Vol. 7, No. 1, 16–32, 2019.
6. Gorrepotu, R., N. S. Korivi, K. Chandu, and S. Deb, "Sub-1 GHz miniature wireless sensor node for IoT applications," *Internet of Things*, Vol. 1, 27–39, 2018.
7. Roges, R., P. K. Malik, and S. Sharma, "A compact CPW-fed log-periodic antenna for IoT applications," *2021 International Conference on Communication, Control and Information Sciences (ICCISc)*, Vol. 1, 1–5, IEEE, June 2021.
8. Chouhan, S., D. K. Panda, and V. S. Kushwah, "Modified circular common element four-port multiple-input-multiple-output antenna using diagonal parasitic element," *International Journal of RF and Microwave Computer-Aided Engineering*, Vol. 29, No. 2, e21527, 2019.
9. Kumar, P., S. Urooj, and A. Malibari, "Design and implementation of quad-element super-wideband MIMO antenna for IoT applications," *IEEE Access*, Vol. 8, 226697–226704, 2020.
10. Kumar, N. and R. Khanna, "A compact multi-band multi-input multi-output antenna for 4G/5G and IoT devices using theory of characteristic modes," *International Journal of RF and Microwave Computer-Aided Engineering*, Vol. 30, No. 1, e22012, 2020.
11. Maurya, N. K. and R. Bhattacharya, "Design of compact dual-polarized multiband MIMO antenna using near-field for IoT," *AEU — International Journal of Electronics and Communications*, Vol. 117, 153091, 2020.
12. Moradi, A., R. Ngah, and M. Khalily, "Polarized diversity compact planar MIMO antenna for wireless access point applications," *Progress In Electromagnetics Research C*, Vol. 91, 115–127, 2019.
13. Malik, P., J. Lu, B. T. P. Madhav, G. Kalkhambkar, and S. Amit, *Smart Antennas: Latest Trends in Design and Application*, Springer, ISBN 978-3-030-76636-8, doi: 10.1007/978-3-030-76636-8, 2021.
14. Malik, P. K., *Planar Antennas: Design and Applications*, Taylor and Francis, ISBN 9781032034461, August 4, 2021.
15. Dkiouak, A., A. Zakriti, and M. El Ouahabi, "Design of a compact dual-band MIMO antenna with high isolation for WLAN and X-band satellite by using orthogonal polarization," *Journal of Electromagnetic Waves and Applications*, Vol. 34, No. 9, 1254–1267, 2020.
16. Kiem, N. K. and D. N. Chien, "A transmission line decoupling technique for enhancement of port isolation of dual-band MIMO antennas," *Journal of Electromagnetic Waves and Applications*, Vol. 32, No. 10, 1195–1211, 2018.
17. Kim, D. W. and S. Nam, "Systematic design of a multiport MIMO antenna with bilateral symmetry based on characteristic mode analysis," *IEEE Transactions on Antennas and Propagation*, Vol. 66, No. 3, 1076–1085, 2017.
18. Yu, K., Y. Li, and X. Liu, "Mutual coupling reduction of a MIMO antenna array using 3-D novel meta-material structures," *The Applied Computational Electromagnetics Society Journal (ACES)*, 758–763, 2018.
19. Khurshid, A., J. Dong, M. S. Ahmad, and R. Shi, "Optimized super-wideband MIMO antenna with high isolation for IoT applications," *Micromachines*, Vol. 13, No. 4, 514, 2022.
20. Rezapour, M., J. Rashed-Mohassel, A. Keshtkar, and M. Naser-Moghadasi, "Isolation enhancement of rectangular dielectric resonator antennas using wideband double slit complementary split ring resonators," *International Journal of RF and Microwave Computer-Aided Engineering*, Vol. 29, No. 7, e21746, 2019.
21. Hu, W., L. Qian, L. Wen, X. Yang, and Y. Yin, "Compact dual-band antenna based on CRLH-TL for WWAN/LTE terminal applications," *International Journal of RF and Microwave Computer-Aided Engineering*, Vol. 29, No. 4, e21587, 2019.

22. Sanad, M. and N. Hassan, "Orthogonally polarized MIMO LTE/5G terminal antennas for handsets and IoT applications," *2019 IEEE Radio and Wireless Symposium (RWS)*, 1–4, IEEE, January 2019.
23. Jha, K. R., B. Bukhari, C. Singh, G. Mishra, and S. K. Sharma, "Compact planar multistandard MIMO antenna for IoT applications," *IEEE Transactions on Antennas and Propagation*, Vol. 66, No. 7, 3327–3336, 2018.
24. Chouhan, S., D. K. Panda, V. S. Kushwah, and P. K. Mishra, "Octagonal-shaped wideband MIMO antenna for human interface device and S-band application," *International Journal of Microwave and Wireless Technologies*, Vol. 11, No. 3, 287–296, 2019.